

## Precise identification of objects in a hyperspectral image by characterizing the distribution of pure signatures

Soumyashree M. Panchal<sup>1</sup>, Shivaputra<sup>2</sup>

<sup>1</sup>Department of Information Science and Engineering, HKBK College Engineering, Bangalore, India

<sup>2</sup>Electronics and Communication Engineering, Dr. Ambedkar Institute of Technology, Bangalore, India

### Article Info

#### Article history:

Received Aug 25, 2021

Revised Jun 21, 2022

Accepted Jul 15, 2022

#### Keywords:

Hyper cube

Hyperspectral image

Object classification

Pixel unmixing

Pure signature

### ABSTRACT

Hyperspectral image (HSI) has been widely adopted in many real-world applications due to its potential to provide detailed information from spectral and spatial data in each pixel. However, precise classification of an object from HSI is challenging due to complex and highly correlated features that exhibit a nonlinear relationship between the acquired spectral unique to the HSI object. In literature, many research works have been conducted to address this problem. However, the problem of processing high-dimensional data and achieving the best resolution factor for any set of regions remains to be evolved with a suitable strategy. Therefore, the proposed study introduces simplified modeling of the hyperspectral image in which precise detection of regions is carried out based on the characterization of pure signatures based on the estimation of the maximum pixel mixing ratio. Moreover, the proposed system emphasizes the pixel unmixing problem, where input data is processed concerning wavelength computation, feature extraction, and hypercube construction. Further, a non-iterative matrix-based operation with a linear square method is performed to classify the region from the input hyperspectral image. The simulation outcome exhibits efficient and precise object classification is achieved by the proposed system in terms classified HSI object and processing time.

*This is an open access article under the [CC BY-SA](https://creativecommons.org/licenses/by-sa/4.0/) license.*



### Corresponding Author:

Soumyashree M. Panchal

Department of Information Science and Engineering, HKBK College Engineering

Bangalore, India

Email: soumya4041@gmail.com

## 1. INTRODUCTION

Hyperspectral imagery (HSI) provides a good scope of in-depth analysis for various remote-sensing domains to understand, identify objects, materials, or trace processes [1]. HSI technology utilizes various spectrometer sensors (such as AVIRIS and ROSIS) to capture views or locations of interest over the wavelength ranges from perceptible to closer infrared [2]. The captured HSI encompasses the rich spectral evidence revealing the exclusive corporal attributes of the ground traits and offers abundant spatial information related to the ground traits [3]. Therefore, HSI is widely used in many real-world applications to obtain thorough spectral evidence and to address problems of discriminating objects that cannot be resolved well through multispectral images. HSI's potential applications include precision agriculture, environment monitoring, atmosphere, ocean, inland waters, ice and snow, medicine, forestry, mine detection, space, and mineral exploration [4], [5]. HSI generally captures more than two hundred contiguous wavelength bands ranging from 0.4 to 2.5  $\mu\text{m}$  and constructs a hypercube that systematically combines the 3D spectral and 2D spatial information, which helps practitioners realize accurate identification and characteristics ground objects [6], [7]. Despite the wide range of information that offers many opportunities, it also comes with

many challenges due to a variety of reasons. First, the captured HSI exhibits the unique statistical and geometric features of high dimensional 3D spectral and 2D spatial data [8]. On the other hand, the hypercube, an n-dimensional hyperspectral object obtained from HSI, may contain less specific information because of non-uniform proportion or distribution of spectral and spatial information and highly correlated adjacent bands [9].

As a result, HSI pixels are most likely to be assorted and mixed with manifold substances [10]. Therefore, mining pure signatures from HIS poses a huge challenge in the process of region classification and analysis. This has led to the research field of spectral unmixing, which can be regarded as a quantitative and measurable analysis to identify pure signature (endmembers) and their mixing ratio (abundance). Extensive research works have been done in the literature to address spectrum unmixing problems based on linear and nonlinear approaches. Nonlinear methods can simulate physical phenomena well, so they can bring better separation or unmixing performance for some applications [11]. Besides, nonlinear methods are usually associated with complex mathematical representations and are applicable to limited applications [12]. In contrast, linear methods are easy to implement and widely adopted in various remote sensing fields. A least square method is one of the popular linear approaches to solve the problem of spectral mixing based on abundance estimation [13].

However, this method is highly dependent on the recognizability conditions, that it needs to process a large number of spectral bands compared to a number of the pure signature. In addition, the highly correlated bands and redundancy in HSI also lead to an increase in computational overhead, which may compromise the performance of the abundance estimation. In this regard, several solutions were introduced in the literature that is generally based on feature extraction and band selection methods. The band selection-based approach is mainly a matter of correlation analysis and computation of shared or common information, whereas feature extraction is mostly done using principal component analysis (PCA), scaling techniques, and linear discriminant analysis (LDA). The work done by Kang *et al.* [14] suggested an HSI classification scheme where attributes were extracted using an edge-aware filter, and its dimensionality is reduced using PCA. The reduced features were then introduced to the SVM classifier to perform HSI classification. Since the HSI data is very complex, highly correlated, and in this study, only spectral features were extracted, which may not provide better feature representation during the training phase, and the classifier may not perform very well. The study of Rajegowda and Balamurugan [15] employed an unsupervised band selection mechanism approach to classifying highly redundant hyperspectral data. Texture analysis is done based on the metric-band similarities and employed the application of kernel-oriented neural networks for the classification. The work of Zhou *et al.* [16] adopted a learning model to address unmixing problems with the matrix factorization technique. In a similar direction, the work of Qi *et al.* [17] presented a solution against unmixing problem based on the sparse matrix representation considering both spatial and spectral data processing.

Chatterjee and Yuen [18] also employed a learning mechanism using a sparse coding dictionary towards achieving higher accuracy in the classification process. In the study of Narmadha *et al.* [19], the authors have focused on the HSI compression using Polyadic decomposition and discrete wavelet transform approach. This approach provides good compression performance but may be subjected to the error of information loss or visual quality in the reconstructed image. The work of Drumetz *et al.* [20] considered the problem of intra-class variability of HSI and introduced an unmixing mechanism based on the group sparsity and mixed norms as an optimization problem. In another study by Wang *et al.* [21], an approach of independent component analysis (ICA) is used to characterize mixing ratio variables, and a gradient descent mechanism is used to classify the HSI regions. In the work of Liu *et al.* [22], spatial structural attributes and statistical information is combined and represented into the positive matrix factorization to handle dynamicity associated with the unmixing process. Salem *et al.* [23] suggested a band selection mechanism oriented on the layer-based spectral and spectrum information using C-means clustering. The work of Wo *et al.* [24] introduced a framework to assess different techniques from different perspectives, such as feature representation and classification performance.

The work of Hossain *et al.* [25] presented a dimension minimization mechanism based on the joint approach of PCA and normalized shared information. Rizkinia and Okuda [26] introduced a regularization algorithm developed based on the nuclear norm using a low-rank local mixing ratio to classify regions in the HSI. Apart from this, there are various other works carried out in the context of spectral unmixing such as sparse regression using learning techniques given by Yuan *et al.* [27], sparse coding mechanism for object extraction by Farani and Rabiee [28], a blind unmixing approach introduced by Yao *et al.* [29]. Hence, there are many research efforts based on the different techniques proposed by the researchers to address the unmixing and region classification in the HSI. However, most of the existing methods are subjected to less accuracy in the precise feature representation. Also, many of the previous works based on the learning techniques may be subjected to the computation overhead and inappropriate classification outcome. The following are the few significant research problem being explored based on the above discussions.

- According to analysis, most existing works only use spectral information in the feature extraction process, so they achieved low performance.
- Also, the adoption of matrix factorization is most dominant in previous research works.
- It has also been found that many research schemes are associated with iterative mechanisms to solve the unmixing problem. However, such approaches are computationally expensive and do not place much focus on classification errors.
- The classification error rests on the fact that it shows an error in the mixing ratio estimation, which is less considered in existing works.

Therefore, the proposed research study intended to present a different solution, unlike existing research works, to address problems of pixel mixing. The proposed scheme aims at classifying the objects in the HSI based on the characterization of pure signature distribution across an identifiable surface in the hyperspectral scene. A set of values for the mixing ratio is obtained for each pixel representing the percentage of each pure signature present in the HSI data with a high spatial correlation to local regions. Further, finding the extreme mixing ratio value for each pixel and assigning it to the corresponding pure signature class. The design consideration of the proposed scheme is based on the different factors viz. i) the statistical dependence of pure signatures should be least correlated, as pure signatures represent different classes, ii) the pure signatures occurrence possibility is usually low, and iii) if they occur then the spatial scope of their occurrences is generally less. In addition, the fully constrained least-squares method (FCLSM) is used to perform material quantification to accurately estimate the maximum size of the true mixing ratio of the sub-pixels contained in the vector. Figure 1 highlights the schematic architecture of the proposed method.

The proposed study presents an analytical model capable of classifying an object from an HSI using a non-recursive and computationally efficient mechanism. The core idea is to estimate the maximum mixing ratio vector corresponding to the pure signature to be set to the particular object class. The systematic processes involved in the proposed methodology are highlighted as follows:

- Indian pine HSI image dataset is considered for the execution of the proposed scheme for HSI classification.
- Wavelength is determined based on the maximum and minimum range of bands provided in the dataset to construct hypercube
- Further, the transformation of the color space is carried out to represent HSI into Red, Green and Blue (RGB) color space. This process helps in dealing with the high dimensionality nature of HSI. It is also further used to represent the final outcome by superimposing the RGB image to the classified object with a pure signature.
- Mixing pixel map is estimated to obtain 3D vector that consists of spatial dimension, and maximum value of mixing pixel is obtained from the 3D vector for each corresponding pure signature pixels
- In the classification phase, the HSI region obtained based on the maximum value of the mixing pixel is then superimposed with the RGB image to interpret the final outcome. The proposed method's design is carried out so that it is more flexible, computationally efficient, and can handle any linear constraint. The next section discusses the methodology adopted in the design implementation of the proposed scheme to address pixel unmixing and classification of the region of highly correlated spectral data.

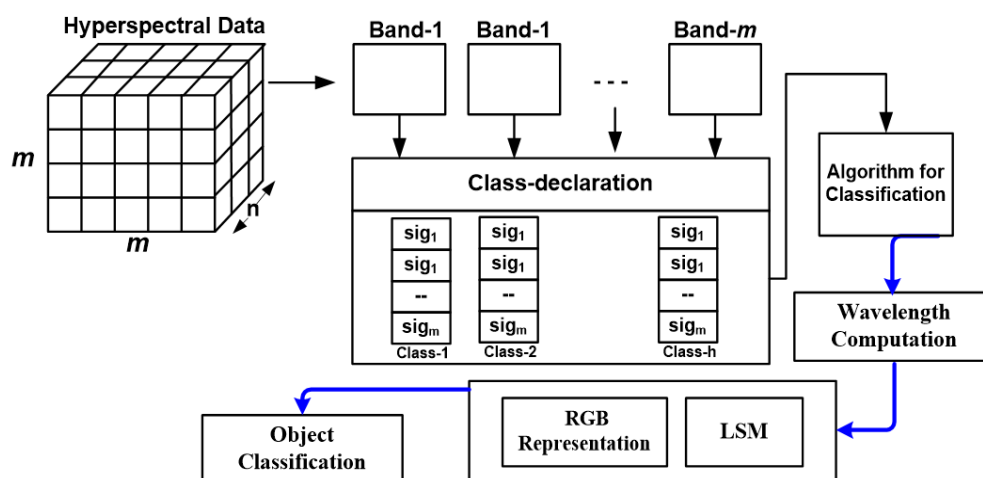


Figure 1. Proposed model of HSI classification

**2. METHOD**

This section discusses the method adopted in implementing the proposed system to address the problem of pixel unmixing (PU) by characterizing the distribution of the pure signature ( $\rho$ ) or endmembers in the HSI region. The initial operation will be to estimate the involved quantity of endmembers which is followed by retrieval of spectral signatures. It should be noted that this extraction is carried out from these endmembers. At the end, the final step will be to evaluate the sufficient availability of each pixel in these endmembers. The process of the pixel decomposition for pixel unmixing SUs is carried out by estimating the maximum value of the proportion of mixing pixel or abundance ( $\alpha$ ) using the least square method (LSM) Figure 2 illustrates pixel mixing context in HIS with its component as abundance and endmember.

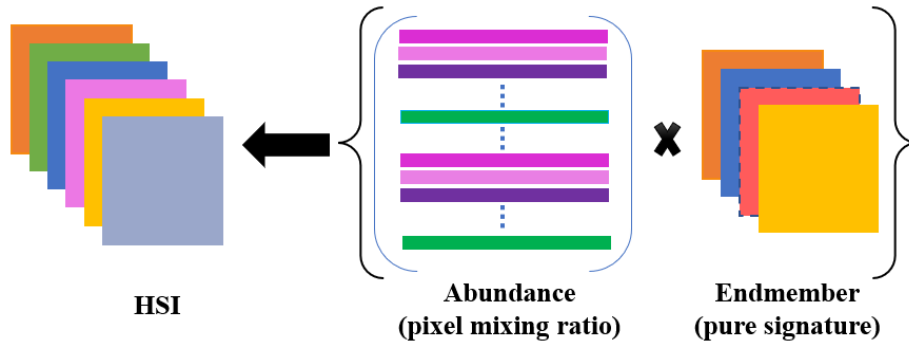


Figure 2. illustration of HSI and component as abundance and endmember

**2.1. Problem formulation**

This section presents a formulation of the problem for unmixing the pixel from the highly correlated HSI image. However, prior to problem formulation, it is essential to describe the notion used in the proposed methodology of HSI object classification. The input HSI  $I_{HS} \in R^{L \times K}$  consists of pixel  $P_x \in R^L$ , where  $\{x = 1, 2, 3, \dots, K\}$  in columns,  $K$  denotes the number of pixels, and  $L$  refers to the number of bands. The pure signature  $\rho_i \{i = 1, 2, 3, \dots, \rho\}$  for PU are arranged in the vector such that  $M \in R^{L \times \rho}$ . Therefore, the estimation of abundance or mixing ratio  $\alpha_{xi} \forall P_x$  and  $\rho_i \in A$  is an  $n$ -dimensional vector such that:  $A \in R^{\rho \times K}$ . Considering these notions, the linear model for addressing SU can be numerically represented as (1):

$$P_x = \sum_{i=1}^{\rho} \alpha_{xi} \cdot M_{\rho} + n_k \tag{1}$$

The matrix representation (1) can be given as (2), (3):

$$I_{HS} = AM + n \tag{2}$$

$$P_x = \begin{bmatrix} 1 \\ 2 \\ \vdots \\ K \end{bmatrix}; A = \begin{bmatrix} \alpha_{11} & \alpha_{12} & \dots & \alpha_{1n} \\ \alpha_{21} & \alpha_{22} & \dots & \alpha_{2n} \\ \vdots & \vdots & \vdots & \vdots \\ \alpha_{m1} & \alpha_{m2} & \dots & \alpha_{mn} \end{bmatrix}; M = \begin{bmatrix} 1 \\ 2 \\ \vdots \\ \rho \end{bmatrix}; n = \begin{bmatrix} n_1 \\ n_2 \\ \vdots \\ n_k \end{bmatrix} \tag{3}$$

where,  $n \in R^{L \times K}$  denotes additive noise in the  $I_{HS}$ . In order to accomplish the goal of determining the maximum value of the  $\alpha$  for the corresponding characterization of  $\rho \forall$  pixel  $P_x$  of  $I_{HS}$  is carried out the considering constraints of the positivity such that  $\alpha \geq 0 \forall P_x, \rho_i$  as (4).

$$(\forall, \rho_i \in \{1, \dots, \rho\})(\forall P_x \in \{1; \dots, K\}) \alpha \geq 0 \tag{4}$$

In (3), the positivity constraint will be denoted as  $\alpha \geq 0$ . Furthermore, considering that all endmembers or pure signature  $\rho$  encompassing  $P_x$  spectrum in  $I_{HS}$  are contained in the column of  $M$ , in this regard, the mixing pixel ratio (abundance)  $\alpha_{xi}$  must meet the criteria of complete additivity constraint such as given in (5):

$$(\rho \in \alpha \forall P_x \in \{1; \dots, K\}) \sum_{i=1}^{\rho} \alpha_{xi} \forall x = 1 \tag{5}$$

However, applying LSM in the pure signature ( $\rho$ ) estimation process, a problem will encounter when the set of  $\rho$  is incomplete and if it is considered that there are  $n$  number of  $\rho$  characterize the mixed pixels in HSI, the target is to compute  $(n - 1)$  subspace, and remaining  $m$ -subspace can be treated as  $n_k$ . But the problem is dealing the least squares and constraints so that estimation can be done in an unbiased manner. Therefore, this problem can be represented as constraint optimization numerically given as (6):

$$\arg \min ||I_{HS} - MA||_{\varphi}^2 \quad (6)$$

where,  $I_{HS}$  denotes HSI,  $M$  denotes column of pure signature ( $\rho$ ) in the matrix,  $A$  denotes  $n$ -dimensional abundance ( $\alpha$ ) vector and  $|| \cdot ||_{\varphi}$  is sub-multiplicative operation refers to vector-norm. Another challenge during HSI region classification is dealing with high dimensionality. In order to handle the imbalance proportion of the samples and complexities poses by the pixel mixing, the proposed study uses the proportion of mixing map to compute the maximum value of  $\alpha \forall$  pixel  $P_x$  and assigning it to the associated  $\rho$  label. At the initial step, the proposed model requires the import of dataset ( $X$ ) to the system to extract HSI intrinsic attributes ( $F_s$ ) that reflect spectral band ( $L$ ), class signature ( $\rho$ ), and a number of bands ( $nL$ ). However, ranges of wavelengths are specified in the adopted HSI dataset. The sequential procedure for classifying different region from HSI is discussed in the following sub-sections.

## 2.2. Implementation

This section discusses the methodology implemented, followed by the algorithmic steps for classifying an object from HSI based on the estimation of the  $\alpha$  vector. An algorithm is formulated that is capable of performing object classification on the basis of specific vector. The complete operation of this algorithm is carried out using matrix-based operation that simplifies the functional steps involved. Further, this algorithm takes the input of dataset which after processing yields to a classified object.

Algorithm-1: classification of an object based on  $\alpha$  vector

**Input:**  $X$  (dataset)

**Output:**  $CL_{obj}$

**Start**

1.  $[F_s, I_{HS}] \leftarrow f_1(X)$   
 $F_s \in \{L, \rho, \lambda_{max}, \lambda_{min}\}$
2. Compute:  $\lambda \forall L$
3. Construct:  $H_c \rightarrow f_2(L, \lambda)$
4. Color space transformation  
 $I_{HS} \text{ to RGB: } I_{RGB} \rightarrow f_3(H_c)$
5. normalize:  $I_{RGB} \rightarrow f_4(I_{RGB})$
6. Visualize: Object class
7. plot  $\leftarrow$  class.lables( $X$ )
8. computation of  $\alpha$  vector  
 $[\bar{\alpha}]_{145 \times 145 \times 16} \leftarrow f_5(H_c, \rho)$
9. Visualize  $[\bar{\alpha}]$
10. compute  $[\bar{\alpha}]_{max} \rightarrow f_{max}([\bar{\alpha}])$
11. Perform:  $Obj_{seg} \rightarrow f_6([\bar{\alpha}]_{max})$
12.  $CL_{obj} \leftarrow$  superimpose( $I_{RGB}, Obj_{seg}$ )

**End**

The above-mentioned computing steps adopt an analytical approach to perform object classification by characterizing the HSI's features set ( $F_s$ ). The first step of the proposed algorithm is to take  $I_{HS}$  and determine the feature set  $F_s$  using function  $f_1$  that takes input argument as a dataset ( $X$ ). This function provides features of the HSI as a set of a number of bands ( $L$ ), pure signature ( $\rho$ ) that reflects Class, and the minimum and maximum wavelength ( $\lambda_{min}$ ) and ( $\lambda_{max}$ ) respectively. In the next step of the algorithm, the value of wavelength ( $\lambda$ ) is computed for all number of bands ( $L$ ) using the given value ( $\lambda_{min}$ ) and ( $\lambda_{max}$ ) numerically expressed as (7):

$$\lambda = \frac{(\lambda_{max} - \lambda_{min})}{L} \quad (7)$$

where,  $\lambda_{max}$  is equal to  $2.5 \mu_m$ ,  $\lambda_{min}$  is equal to  $0.4 \mu_m$  and  $L$  is number of spectral band equal to 220.

Figure 3 represents a sample visualization of the wavelength over 120 spectral bands. The characteristics of the dataset are represented in Table 1. Further, in the next step, the study computes hypercubic objects using function  $f_2$  that creates a hypercubic object  $H_c$  by taking input argument as  $L$  and

value of  $\lambda$ . As a result, the  $H_c$  consists of both spectral and spatial information of the HSI image with L bands. Further, the visualization of the image in RGB color space is carried out using function  $f_3$  that takes input value as  $H_c$ . This function performs colorization over the hypercubic objects and provides the image in the RGB color representation, which is further normalized and enhanced using function  $f_4$  that denotes contrast stretching mechanism numerically expressed as (8):

$$I_{rgb_{norm}} = (I_{rgb} - c) \left( \frac{b-a}{d-c} \right) + a \tag{8}$$

where,  $P_{out}$  normalized and enhanced image,  $P_{in}$  denotes input image, a and b denotes lower and upper limit, where c and d are the existing lower- and upper-pixel values in the input image. The value ranges between [0, 255]. Figure 4 illustrates the representation of the HSI in RGB color space.

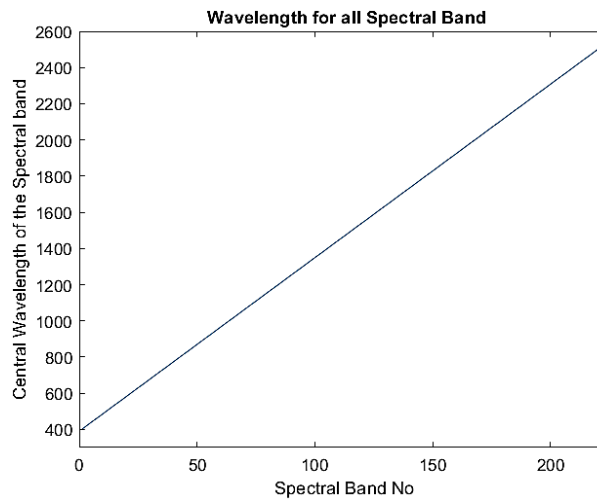


Figure 3. Wavelength of each spectral band (Sb)

Table 1. Characterization of hypercubic HSI object

No. of spectral band (nSb)	Wavelength range (Wr in nm)	Geometric resolution (Gr in m)	Spatial resolution (Sr in pixel) dimension
220	0.4-2.5	1.3	145x145



Figure 4. Representation of  $H_c$  information in the RGB color space

The visualization of the hypercubic HSI object is shown in Table 2 with a total of '16' classes and a corresponding number of the samples. After visualizing the class of objects in the dataset, the algorithm then computes the vector as an abundance-map using function  $f_5$  that takes input values as  $H_c$  and  $\rho$ . Here the

function  $f_5$  denotes a mechanism of FCLSM to estimate the  $\alpha$  for each  $\rho$  corresponding to the HSI pixel. The obtained outcome is achieved in the form of a vector such that  $\overline{[\alpha]}$  with dimension  $m \times n \times C$ , where  $m$  denotes the row and  $n$  denotes column and  $c$  denotes number classes. It can be observed from Table 1 that the size of  $n$  and  $m$  are  $145 \times 145$ , and total number of class  $C$  is equal to 16. Figure 5 depicts the visualization of pixel mixing proportion for all pure signature of class.

Table 2. Ground truth classes with respective samples number

Class	No. of Samples	Class	No. of Samples	Class	No. of Samples
C1	Alfalfa-46	C7	Grass-pasture mowed 28	C13	Wheat 205
C2	Corn-notill 1428	C8	Hay-windrowed 478	C14	Woods 1265
C3	Corn-mintill 830	C9	Oats 20	C15	Buildings Grass Tree Drives 386
C4	Corn 237	C10	Soybean-notill	C16	Stone-Steel-Towers93
C5	Grass-pasture 483	C11	Soybean mintill 2455		
C6	Grass-trees 730	C12	Soybean-clean 593	Total Class	16

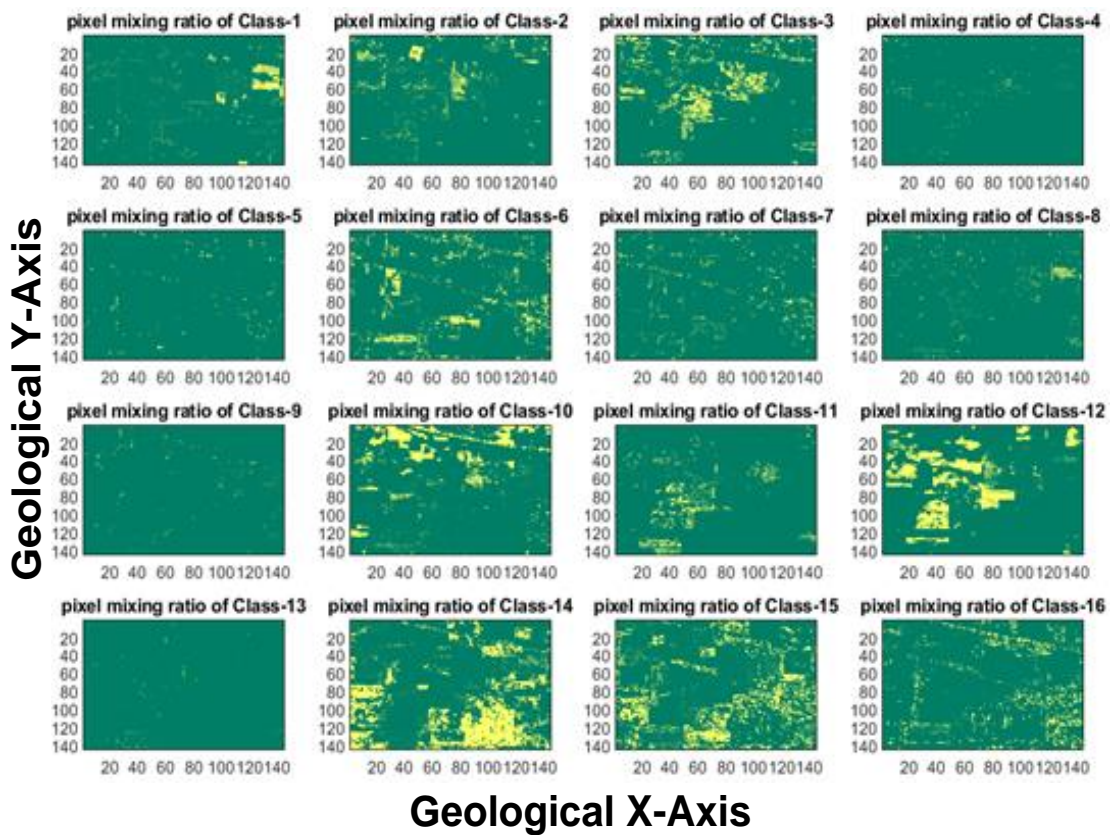


Figure 5. Pixel mixing ratio map

From Figure 5, it can be analyzed that mixing pixel signifies the inherent features of the spectral of the multiclass, i.e., linearly correlated with the pure signature represents a unique class of objects. In order to perform object classification, the study performs the computation of the maximum value present in the  $\overline{[\alpha]}_{\max}$ . Therefore, a function  $f_{\max}$  is used to compute the maximum mixing ratio, i.e.,  $\overline{[\alpha]}_{\max}$ , which then used to perform segmentation of objects from HSI using function  $f_6$ . In this process, indices are computed corresponding to the largest mixing pixel ratio vector for every pixel that belongs to the pure signature. In Figure 6 heat map is shown for the pure signature identified based on the maximum value of the mixing pixel. Further, the function  $f_6$  is used to construct a matrix of zero having a dimension equal to the  $\overline{[\alpha]}_{\max}$ , so that the final version of segment or classified objected is obtained efficiently. In this process, the previously computed RGB image is then superimposed to  $Obj_{\text{seg}}$ . Based on the mapping function of the binary mask, the classified object of HSI is superimposed with the RGB image with the pure color code.

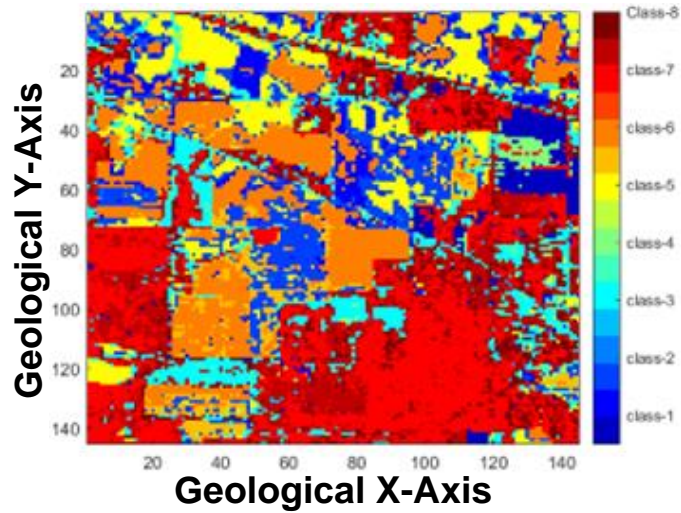


Figure 6. Heat map of objects or region

### 3. RESULTS AND DISCUSSION

This section discusses the outcome and performance analysis of the proposed system in terms of processing time. The overall design and implementation of the proposed study is carried out on the numerical computing environment (MATLAB). Moreover, the execution of the proposed work is carried out considering a typical Indian pine HIS dataset. Figure 7 illustrates the mapped classification representation with the HSI zones along with the class labels.

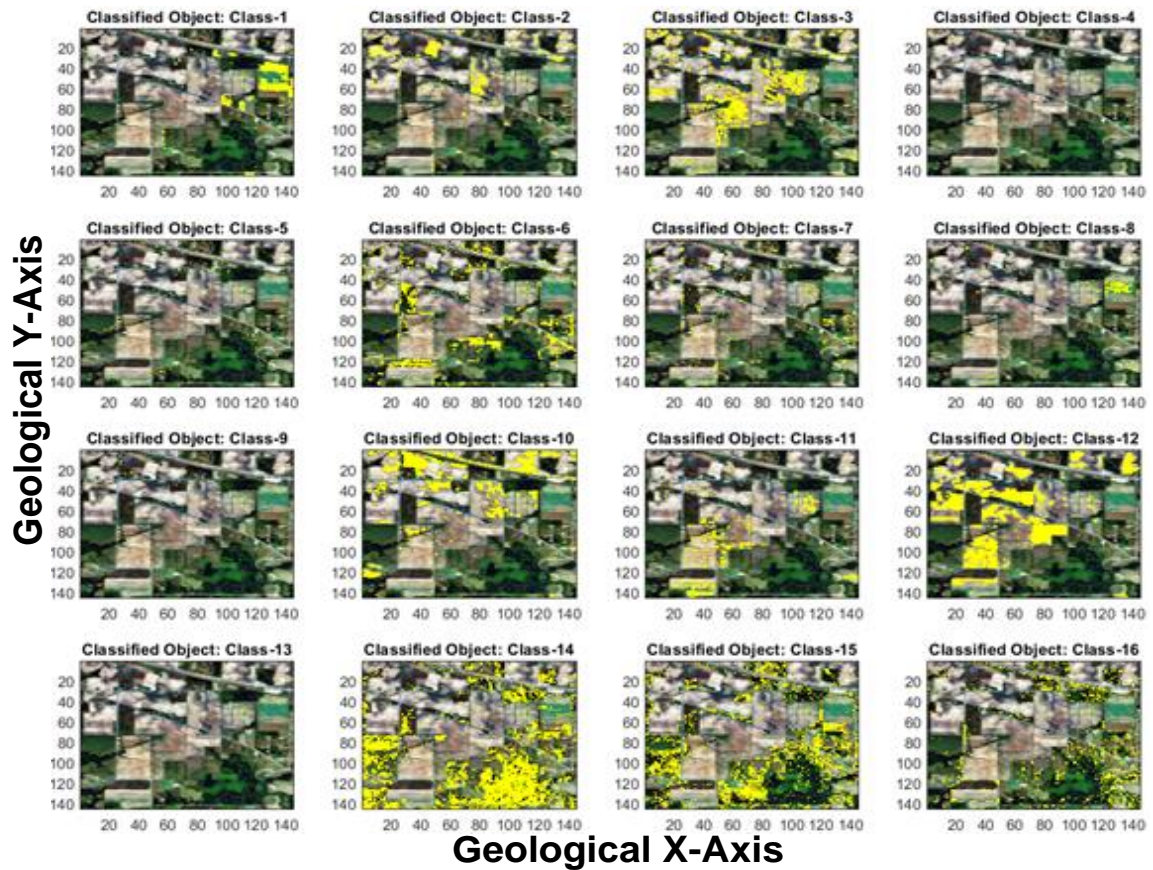


Figure 7. Classified region



Figure 7 shows the final outcome as classified objected from the HIS image based on the characterization of the pure signature and mixing pixel ratio map. The next analysis is carried out to justify the effectiveness and scope of the proposed study based on the comparative analysis considering similar existing research works carried out by Sun *et al.* [30] (Exist1) and Sun *et al.* [31] (Exist2). In the work of Sun *et al.* [30], the authors have considered the separability of spectral bands based on the nonnegative matrix factorization to preserve the quantitative spectral information spectral data. In this study, the selection of spectral bands is associated with uncertainties due to arbitrary initialization in the clustering operation. The work carried out by Sun *et al.* [31] presented an approach of band selection based on the sparse representation mechanism to hold appropriate visual information for the chosen bands. However, the presented approach is effective, but it lacks minimum noise band selection and is not much suitable when dealing with highly noisy HSI bands in the real-time scenario. From Figure 8, it can be analyzed that the methodology adopted in the proposed study provides better outcomes regarding object classification and has reduced processing time which shows its cost-efficiently in a run time environment. The proposed methodology involved a sophisticated procedure, unlike conventional methods to address pixel mixing problems.

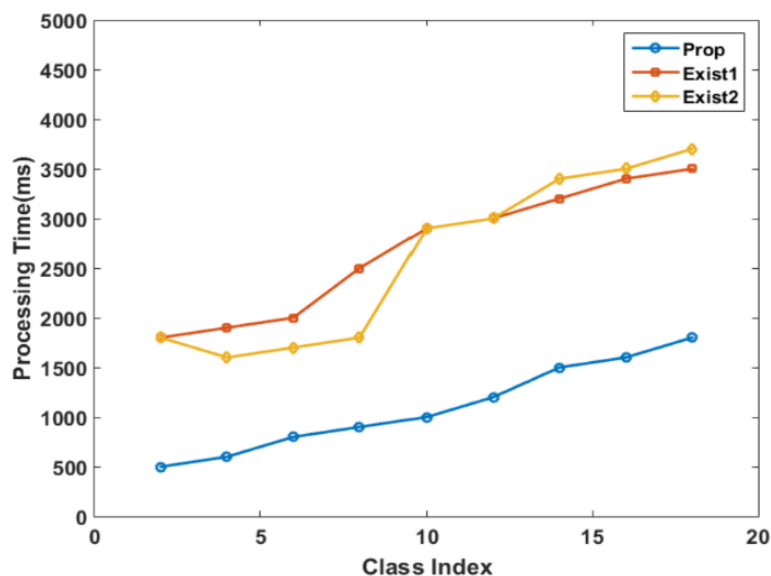


Figure 8. Analysis of processing time

#### 4. CONCLUSION

Hyperspectral images deliver abundant evidence about the scene captured than the other imaging methods. However, due to intra-class variability and spatial constraint resolution, HSI pixels are most likely to be assorted and mixed with manifold substances. Therefore, the proposed study aimed to address pixel unmixing and estimation of pure signature with their mixing ratio in each pixel unique to the corresponding class. The execution of the current research study is carried out considering hyperspectral images from the Indian Pine dataset. The implementation of the methodology adopted computationally efficient strategies, where at beginning features of the hyperspectral dataset are computed to construct hypercube object that consists of both spectral and spatial visual information and the number of bands. In order to handle the high dimensionality problem, the study performs construction of visual scene or observation in the RGB from the hypercube, which is then normalized using point operation. The operations, i.e., estimation of pure signature and pixel mixing ratio vectors, are carried out using non-iterative matrix-computation. The classified object is then superimposed with the RGB images to construct the final outcome. The design and implementation of the proposed system are carried out on the numerical computing tool (MATLAB). The simulation outcome exhibited that the proposed system has achieved better performance regarding object classification. The effectiveness and scope of the proposed system are justified based on the comparison analysis with the similar existing techniques in terms of processing time. Also, the methodology adopted in the proposed study can handle any linear constraint; therefore, it is more flexible and computationally efficient than the existing methods.




## REFERENCES

- [1] M. J. Khan, H. S. Khan, A. Yousaf, K. Khurshid, and A. Abbas, "Modern trends in hyperspectral image analysis: A review," *IEEE Access*, vol. 6, pp. 14118–14129, 2018, doi: 10.1109/ACCESS.2018.2812999.
- [2] S. Jeyakumar and S. Sudha, "Hybrid hyperspectral image compression technique for non-iterative factorized tensor decomposition and principal component analysis: application for NASA's AVIRIS data," *Computational Geosciences*, vol. 23, no. 5, pp. 969–979, Oct. 2019, doi: 10.1007/s10596-019-09855-2.
- [3] K. S. He, D. Rocchini, M. Neteler, and H. Nagendra, "Benefits of hyperspectral remote sensing for tracking plant invasions," *Diversity and Distributions*, vol. 17, no. 3, pp. 381–392, May 2011, doi: 10.1111/j.1472-4642.2011.00761.x.
- [4] B. Park and R. Lu, *Hyperspectral imaging technology in food and agriculture*. New York, NY: Springer New York, 2015.
- [5] D. Wu and D.-W. Sun, "Advanced applications of hyperspectral imaging technology for food quality and safety analysis and assessment: A review-Part I: Fundamentals," *Innovative Food Science & Emerging Technologies*, vol. 19, pp. 1–14, Jul. 2013, doi: 10.1016/j.ifset.2013.04.014.
- [6] M. Imani and H. Ghassemian, "An overview on spectral and spatial information fusion for hyperspectral image classification: Current trends and challenges," *Information Fusion*, vol. 59, pp. 59–83, Jul. 2020, doi: 10.1016/j.inffus.2020.01.007.
- [7] A. Mookambiga and V. Gomathi, "Comprehensive review on fusion techniques for spatial information enhancement in hyperspectral imagery," *Multidimensional Systems and Signal Processing*, vol. 27, no. 4, pp. 863–889, Oct. 2016, doi: 10.1007/s11045-016-0415-2.
- [8] B. Boldrini, W. Kessler, K. Rebner, and R. W. Kessler, "Hyperspectral imaging: A review of best practice, performance and pitfalls for in-line and on-line applications," *Journal of Near Infrared Spectroscopy*, vol. 20, no. 5, pp. 483–508, Oct. 2012, doi: 10.1255/jnirs.1003.
- [9] C.-I. Chang, M. Song, J. Zhang, and C.-C. Wu, "Editorial for special issue 'hyperspectral imaging and applications,'" *Remote Sensing*, vol. 11, no. 17, Aug. 2019, doi: 10.3390/rs11172012.
- [10] W. Lv and X. Wang, "Overview of hyperspectral image classification," *Journal of Sensors*, vol. 2020, pp. 1–13, Jul. 2020, doi: 10.1155/2020/4817234.
- [11] S. Chakravorty and D. Sinha, "Analysis of multiple scattering of radiation amongst end members in a mixed pixel of hyperspectral data for identification of mangrove species in a mixed stand," *Journal of the Indian Society of Remote Sensing*, vol. 43, no. 3, pp. 559–569, Sep. 2015, doi: 10.1007/s12524-014-0437-x.
- [12] N. Dobigeon, Y. Altmann, N. Brun, and S. Moussaoui, "Linear and nonlinear unmixing in hyperspectral imaging," *Linear and Nonlinear Unmixing in Hyperspectral Imaging*, vol. 30, pp. 185–224, 2016, doi: 10.1016/B978-0-444-63638-6.00006-1.
- [13] D. C. Heinz and C.-I. Chang, "Fully constrained least squares linear spectral mixture analysis method for material quantification in hyperspectral imagery," *IEEE Transactions on Geoscience and Remote Sensing*, vol. 39, no. 3, pp. 529–545, Mar. 2001, doi: 10.1109/36.911111.
- [14] X. Kang, X. Xiang, S. Li, and J. A. Benediktsson, "PCA-based edge-preserving features for hyperspectral image classification," *IEEE Transactions on Geoscience and Remote Sensing*, vol. 55, no. 12, pp. 7140–7151, Dec. 2017, doi: 10.1109/TGRS.2017.2743102.
- [15] P. M. Rajegowda and P. Balamurugan, "A neural network approach to identify hyperspectral image content," *International Journal of Electrical and Computer Engineering (IJECE)*, vol. 8, no. 4, pp. 2115–2125, Aug. 2018, doi: 10.11591/ijece.v8i4.pp2115-2125.
- [16] L. Zhou *et al.*, "Subspace structure regularized nonnegative matrix factorization for hyperspectral unmixing," *IEEE Journal of Selected Topics in Applied Earth Observations and Remote Sensing*, vol. 13, pp. 4257–4270, 2020, doi: 10.1109/JSTARS.2020.3011257.
- [17] L. Qi, J. Li, Y. Wang, Y. Huang, and X. Gao, "Spectral-spatial-weighted multiview collaborative sparse unmixing for hyperspectral images," *IEEE Transactions on Geoscience and Remote Sensing*, vol. 58, no. 12, pp. 8766–8779, Dec. 2020, doi: 10.1109/TGRS.2020.2990476.
- [18] A. Chatterjee and P. W. T. Yuen, "Sample selection with SOMP for robust basis recovery in sparse coding dictionary learning," *IEEE Letters of the Computer Society*, vol. 2, no. 3, pp. 28–31, Sep. 2019, doi: 10.1109/LOCS.2019.2938446.
- [19] D. Narmadha, K. Gayathri, K. Thilagavathi, and N. S. Basha, "An optimal HSI image compression using DWT and CP," *International Journal of Electrical and Computer Engineering (IJECE)*, vol. 4, no. 3, pp. 411–421, Jun. 2014, doi: 10.11591/ijece.v4i3.6326.
- [20] L. Drumetz, T. R. Meyer, J. Chanussot, A. L. Bertozzi, and C. Jutten, "Hyperspectral image unmixing with endmember bundles and group sparsity inducing mixed norms," *IEEE Transactions on Image Processing*, vol. 28, no. 7, pp. 3435–3450, Jul. 2019, doi: 10.1109/TIP.2019.2897254.
- [21] N. Wang, B. Du, L. Zhang, and L. Zhang, "An abundance characteristic-based independent component analysis for hyperspectral unmixing," *IEEE Transactions on Geoscience and Remote Sensing*, vol. 53, no. 1, pp. 416–428, Jan. 2015, doi: 10.1109/TGRS.2014.2322862.
- [22] R. Liu, B. Du, and L. Zhang, "Hyperspectral unmixing via double abundance characteristics constraints based NMF," *Remote Sensing*, vol. 8, no. 6, May 2016, doi: 10.3390/rs8060464.
- [23] M. Ben Salem, K. S. Ettabaa, and M. S. Bouhlel, "Hyperspectral image feature selection for the fuzzy c-means spatial and spectral clustering," in *2016 International Image Processing, Applications and Systems (IPAS)*, Nov. 2016, pp. 1–5, doi: 10.1109/IPAS.2016.7880114.
- [24] B. Wu, C. Chen, T. M. Kechadi, and L. Sun, "A comparative evaluation of filter-based feature selection methods for hyperspectral band selection," *International Journal of Remote Sensing*, vol. 34, no. 22, pp. 7974–7990, Nov. 2013, doi: 10.1080/01431161.2013.827815.
- [25] M. A. Hossain, X. Jia, and M. Pickering, "Subspace detection using a mutual information measure for hyperspectral image classification," *IEEE Geoscience and Remote Sensing Letters*, vol. 11, no. 2, pp. 424–428, Feb. 2014, doi: 10.1109/LGRS.2013.2264471.
- [26] M. Rizkinia and M. Okuda, "Joint local abundance sparse unmixing for hyperspectral images," *Remote Sensing*, vol. 9, no. 12, Nov. 2017, doi: 10.3390/rs9121224.
- [27] Y. Yuan, Y. Feng, and X. Lu, "Projection-based NMF for hyperspectral unmixing," *IEEE Journal of Selected Topics in Applied Earth Observations and Remote Sensing*, vol. 8, no. 6, pp. 2632–2643, Jun. 2015, doi: 10.1109/JSTARS.2015.2427656.
- [28] A. Soltani-Farani and H. R. Rabiee, "When pixels team up: Spatially weighted sparse coding for hyperspectral image classification," *IEEE Geoscience and Remote Sensing Letters*, vol. 12, no. 1, pp. 107–111, Jan. 2015, doi: 10.1109/LGRS.2014.2328319.
- [29] J. Yao, D. Meng, Q. Zhao, W. Cao, and Z. Xu, "Nonconvex-sparsity and nonlocal-smoothness-based blind hyperspectral




- unmixing,” *IEEE Transactions on Image Processing*, vol. 28, no. 6, pp. 2991–3006, Jun. 2019, doi: 10.1109/TIP.2019.2893068.
- [30] W. Sun, L. Tian, Y. Xu, D. Zhang, and Q. Du, “Fast and robust self-representation method for hyperspectral band selection,” *IEEE Journal of Selected Topics in Applied Earth Observations and Remote Sensing*, vol. 10, no. 11, pp. 5087–5098, Nov. 2017, doi: 10.1109/JSTARS.2017.2737400.
- [31] W. Sun, L. Zhang, B. Du, W. Li, and Y. Mark Lai, “Band selection using improved sparse subspace clustering for hyperspectral imagery classification,” *IEEE Journal of Selected Topics in Applied Earth Observations and Remote Sensing*, vol. 8, no. 6, pp. 2784–2797, Jun. 2015, doi: 10.1109/JSTARS.2015.2417156.

## BIOGRAPHIES OF AUTHORS



**Soumyashree M. Panchal**    pursuing PhD in Dr. AIT, Bangalore, India. She has completed B. E in the Department of ISE, AIET Kalaburagi, Karnataka and M.Tech in CSE VTU Kalaburagi, Karnataka, India. She is having 5 years of experience in the academic. Her research area is image processing using machine learning. She can be contacted at email: soumya4041@gmail.com.



**Shivaputra**    Obtained his B.E. in Electronics & Communication Engineering from University of Visvesvaraya College of Engineering, Bangalore, and Bangalore University in 2002, and M.Tech. Degree in VLSI Design & Embedded System from the BMS College Engineering, Visvesvaraya Technological University in 2009 and PhD from Jain University, Bangalore during 2017. He is a reviewer of The Journal of Supercomputing, springer and several Journal of international repute. He has published more than 18 research papers in the journals of international repute. Under his Guidance 8 M.Tech. Degrees are awarded and working as editorial member of international and national journals. He can be contacted at email: putrauvce@gmail.com.